

RESEARCH

Open Access



# The catabolic nature of fermentative substrates influences proteomic rewiring in *Escherichia coli* under anoxic growth

Huda Momin<sup>1</sup>, Deepti Appukuttan<sup>1</sup> and K. V. Venkatesh<sup>1\*</sup>

## Abstract

**Background** During anaerobic batch fermentation of substrates by *Escherichia coli*, there is a decline in cell proliferation rates and a huge demand is placed on cellular proteome to cater to its catabolic and anabolic needs under anoxic growth. Considering cell growth rates as a physiological parameter, previous studies have established a direct relationship between *E. coli* growth rate and cellular ribosomal content for fast-proliferating cells. In this study, we integrated experimental findings with a systemic coarse-grained proteome allocation model, to characterize the physiological outcomes at slow growth rate during anaerobic fermentative catabolism of different glycolytic and non-glycolytic substrates.

**Results** The anaerobic catabolism of substrates favored high ribosomal abundances at lower growth rates. Interestingly, a modification of the previously discussed “growth law”, the ratio of active to inactive ribosomal proteome was found to be linearly related to the growth rate for cells proliferating at slow to moderate regime (growth rate  $< 0.8 \text{ h}^{-1}$ ). Also, under nutrient- and oxygen-limiting growth conditions, the proteome proportion allocated for ribosomal activity was reduced, and the resources were channelized towards metabolic activities to overcome the limitations imposed during uptake and metabolizing substrate. The energy-intensive uptake mechanism or lower substrate affinity, expended more catabolic proteome, which reduced its availability to other cellular functions.

**Conclusions** Thus, the nature of catabolic substrates imposed either uptake limitation or metabolic limitation coupled with ribosomal limitation (arising due to anoxic and nutritional stress), which resulted in higher proteome expenditure leading to sub-optimal growth phenotype. This study can form the basis for analyzing *E. coli*'s ability to optimize metabolic efficiency under different environmental conditions- including stress responses. It can be further extended to optimizing the industrial anaerobic conversions for improving productivity and yield.

**Keywords** Substrate, Fermentation, Catabolism, Ribosome, Proteome

\*Correspondence:

K. V. Venkatesh  
venks@iitb.ac.in

<sup>1</sup>Department of Chemical Engineering, Indian Institute of Technology  
Bombay, Mumbai 400076, India



© The Author(s) 2025. **Open Access** This article is licensed under a Creative Commons Attribution-NonCommercial-NoDerivatives 4.0 International License, which permits any non-commercial use, sharing, distribution and reproduction in any medium or format, as long as you give appropriate credit to the original author(s) and the source, provide a link to the Creative Commons licence, and indicate if you modified the licensed material. You do not have permission under this licence to share adapted material derived from this article or parts of it. The images or other third party material in this article are included in the article's Creative Commons licence, unless indicated otherwise in a credit line to the material. If material is not included in the article's Creative Commons licence and your intended use is not permitted by statutory regulation or exceeds the permitted use, you will need to obtain permission directly from the copyright holder. To view a copy of this licence, visit <http://creativecommons.org/licenses/by-nc-nd/4.0/>.

## Background

In a single-cell organism like *Escherichia coli*, the strategic allocation of cellular resources rewires physiological outcomes, fundamentally measured as cell proliferation rate under different growth conditions [1–4]. Also, the nutritional content of the growth medium influences cellular gene expression level and its macromolecular composition by orchestrating its growth rate [4–6]. The native host metabolism uniquely metabolizes incoming substrates, for the production of anabolic precursors and energy; thereby leading to polymerization of cellular macromolecules like protein, RNA, cell envelop, etc., in cellular machinery [7]. Within a fixed cellular budget, a bacterial cell balances the production of proteins and their synthesizing machinery called ribosomal assembly [3]. Altogether, the cellular ribosomes are critical in shaping its protein repertoire and the level of gene expression under different growth conditions [4, 8]. The cellular ribosome abundance is reflected by the total RNA-to-protein ( $\frac{R}{P}$ ) ratio, as *E. coli* rRNA (~85% of total RNA) is folded in ribosomes [4, 9] and >95% of total RNA (including rRNAs and tRNAs) deals with protein translation [3, 5]. Moreover, *E. coli* ribosomes exhibit a distinctive mass composition of RNA and protein in a ratio of 2:1, unique for cell growth maximization [10, 11].

The empirical linear relationship between ribosomal abundance and growth rate for *E. coli* cells proliferating in fast to moderately slow regime (doubling time ~20 min to 2 h) [4, 5, 12, 13] has been physiologically defined as the “growth laws” [4, 9]. In a batch culture with limited ribosomes translating at a constant rate, the *E. coli* growth rate can be adjusted by modulating medium composition, such as by adding supplements like amino acids, vitamins, and nucleosides, or altering the carbon source, which favors shorter doubling time and faster proliferation rates. Conversely, when the ribosomal translation rate is impaired by antibiotics in a graded manner in a medium with fixed nutrient composition, there is a decline in growth rate with an increase in ribosomal abundance [4, 8]. This relationship can be improved by enhancing the nutrient medium quality. In both cases, the nutrient medium quality can be critical in defining the physiological outcome. Furthermore, integrating these key observations on ribosome-growth rate relationships with coarse-grained proteome partitioning [4] based on functionality, enhances our understanding of *E. coli* physiology. The studies including specific protein abundance maps and system-wide proteome allocation under different growth conditions have been previously reported [14–16]. The ubiquitous microbial phenomena such as overflow metabolism [17] or carbon catabolite repression [1] has been well explained by considering the cost of protein synthesis. The knowledge of cellular

proteomes has been integrated with a systemic approach to uncover the physiological variations of *E. coli* [18–21]. However, there exists a knowledge gap regarding the resource rewiring in *E. coli* during anaerobic fermentative substrate catabolism.

The anaerobic fermentation is an independent nutritional mode exhibited by *E. coli* cells for the catabolism of different substrates. Although the mode of nutrition has certain limitations in terms of energy biogenesis, substrate oxidation, carbon wastage, etc., it is an appealing mode for the production of various chemicals of industrial significance. So, here we are interested in understanding the role of ribosomes in determining bacterial growth rate during anaerobic fermentative breakdown of different substrates. We also studied the rewiring of proteome allocation with changing substrates and growth rates during anaerobic batch fermentation. Here, we considered six substrates viz., glucose, fructose, xylose, sorbitol, gluconate, and pyruvate, which varied in their chemical nature including carbon content, catabolic pathways, and oxidation state. For understanding the influence of substrate in proteome allocation in *E. coli*, we cultivated cells in minimal growth M9 medium, to rule out the interventions of growth medium in physiological outcome. We resorted to theoretical simulations by constraining the experimental results to generate a coarse-grained model of proteome allocation. Thus, we elucidated the role of ribosomes and proteome partitioning in defining *E. coli* physiology during anaerobic fermentation of different substrates.

## Methods

### The anaerobic batch fermentation

The *Escherichia coli* K-12 strain BW25113 [ $\Delta(araD-araB)567 \Delta(rhaD-rhaB)568 \Delta lacZ4787 (::rrnB-3) hsdR514 rph-1$ ] [22] was used for anaerobic fermentation of different substrates. The bacterial cells were anaerobically cultured at 37 °C, with rotor speed at 120 rpm, in 200 mL sterile M9 minimal medium (composition per litre: 6 g anhydrous  $Na_2HPO_4$ , 3 g  $KH_2PO_4$ , 0.5 g NaCl, 1 g  $NH_4Cl$ , 1 M  $MgSO_4$ , 1 M  $CaCl_2$ ) supplemented with 100 mM MOPS (3-(N-morpholino) propane sulfonic acid) as a buffering agent. The pH of the medium was set to 7.2 and the anaerobic condition was maintained by sparging sterile nitrogen gas in the reaction assembly. The six substrates viz., glucose (2 g  $L^{-1}$ ), fructose (2 g  $L^{-1}$ ), xylose (2 g  $L^{-1}$ ), sorbitol (2 g  $L^{-1}$ ), gluconate (2.4 g  $L^{-1}$ ), and pyruvate (2.4 g  $L^{-1}$ ) were added such that equal amount of carbon was maintained under different growth conditions. The chemicals used in this study were purchased from Merck. The bacterial growth rate was determined spectrophotometrically (Thermo Scientific Multiscan GO) by measuring cellular density at 600 nm ( $O.D_{600}$ ).

### Total RNA estimation by the TRIzol method

Total RNA quantification from three biological replicates for each substrate was done by the TRIzol method [23] with slight modifications. The bacterial cells were harvested from a mid-exponential phase culture of anaerobic fermentation with an optical density of 20 by centrifuging it at 7000 rpm, 4 °C for 20 min. The cell pellet was washed with M9 + MOPS medium, snap-frozen in liquid nitrogen and stored in a -80 °C freezer until RNA extraction. For extracting total RNA, the cells were suspended in 250 µL TRIzol reagent and were homogenized with a sterile micropestle for 1.5 min, this process was repeated twice. Additionally, 500 µL TRIzol reagent was introduced in the centrifuge tube and the suspension was homogenized by vortexing briefly (~15–30 s), followed by incubation at room temperature for 5–7 min for complete dissociation of nucleoproteins complex. Next, 300 µL of chilled chloroform was added to the tube, mixed thoroughly by shaking and incubated for 5 min. The samples were then centrifuged at 13,500 rpm, 4 °C for 20 min. The upper aqueous phase was carefully transferred into a fresh micro-centrifuge tube and 800 µL of chilled isopropanol was added to it. It was then incubated at -20 °C overnight. The next day, the samples were centrifuged at 13,500 rpm, 4 °C for 30 min, forming a white pellet. This pellet was washed twice with 1 mL of 75% chilled ethanol. The pellet was air-dried until translucent. The resulting pellet was suspended in 20 µL nuclease-free water and incubated at a 55 °C dry bath for 10–13 min. The concentration along with purity was checked using nanodrop and the quality check was done by agarose gel electrophoresis. Any genomic DNA contamination in the extracted total RNA was removed by DNase treatment, followed by phenol-chloroform extraction.

### Total protein estimation by the Biuret test

For the Biuret method [1] of total protein quantification, cells from mid-exponential phase culture with an optical density of 2 were collected by centrifuging at 7500 rpm, 4 °C, 20 min. The resulting pellet was washed with autoclaved Milli Q and resuspended in 200 µL water. It was fast-frozen in liquid nitrogen and thawed in a water bath at room temperature for 5 min. 100 µL of 3 M NaOH was added to the samples and it was incubated at 100 °C heat block for 5 min, for protein hydrolysis. The resulting samples were cooled in a water bath at room temperature for 5 min. Later, 100 µL of 1.6% CuSO<sub>4</sub> solution was added, followed by thorough mixing at room temperature for 5 min. Finally, the samples were centrifuged and the absorbance was measured at 555 nm [1]. The protein concentration in the sample was quantified from the BSA standard curve, prepared by the same biuret reaction.

### Genome-scale metabolic model (GEM) and constrained allocation flux balance analysis (CAFBA)

The genome-scale metabolic model *iJO1366* [24] for *E. coli* MG1655 (*E. coli* K-12 family) was used for all simulations with certain modifications unique to the *E. coli* BW25113 strain. The *E. coli* strain BW25113 differs from MG1655 with several gene deletions like *lacZ*, *araBAD*, and *rhaBAD*. Consequently, the fluxes across reactions like LACZ, RMK, RMI, RBK\_L1, RMPA, LYXI, and ARAI were constrained to zero. Moreover, the oxygen exchange reaction was constrained to zero, for mimicking the anaerobic fermentative growth. Constrained Allocation Flux Balance Analysis [19] was used to systematically allocate *E. coli* proteome resources into coarse-grained functional sectors. These sectors comprise genes of common interests such as substrate catabolism, anabolism, housekeeping, maintenance [1, 4], etc. The CAFBA simulations were performed in MATLAB (The MathWorks Inc., MA, USA) using Gurobi Solver (Gurobi Optimization, USA). For our nutrient-limited study, we have systematically categorized the *E. coli* BW25113 proteome into four coarse-grained sectors as:

1. Ribosomal (R) sector ( $\varnothing_R$ ): This class comprises ribosomal and its affiliated proteins.
2. Catabolic (C) sector ( $\varnothing_C$ ): It includes substrate influx and transport proteins.
3. Metabolic (M) sector ( $\varnothing_M$ ): This class accommodates metabolic enzymes.
4. Housekeeping (Q) sector ( $\varnothing_Q$ ): It comprises the growth-independent core proteome.

The fractional proteome share of each sector is represented by  $\varnothing_X$ , where  $X \in (R, C, M, Q)$  respectively.

### Statistical analysis

The results reported here are the mean of three independent biological replicates ( $n=3$ ), represented along standard deviations. The Student's T-test was performed to determine the statistical significance across different growth conditions. Since the experiments were carried out in triplicates, simulations were run thrice for each case to minimize theoretically associated errors. The corresponding deviations are reported along with actual values.

## Results

### The inactive ribosomal abundance influenced total protein content across different growth conditions

The cellular ribosomal abundance determines its protein content. We measured the cellular RNA-to-protein ratio ( $\frac{R}{P}$  ratio,  $r$ ) or ribosomal abundance during anaerobic fermentation of glucose, fructose, xylose, sorbitol,

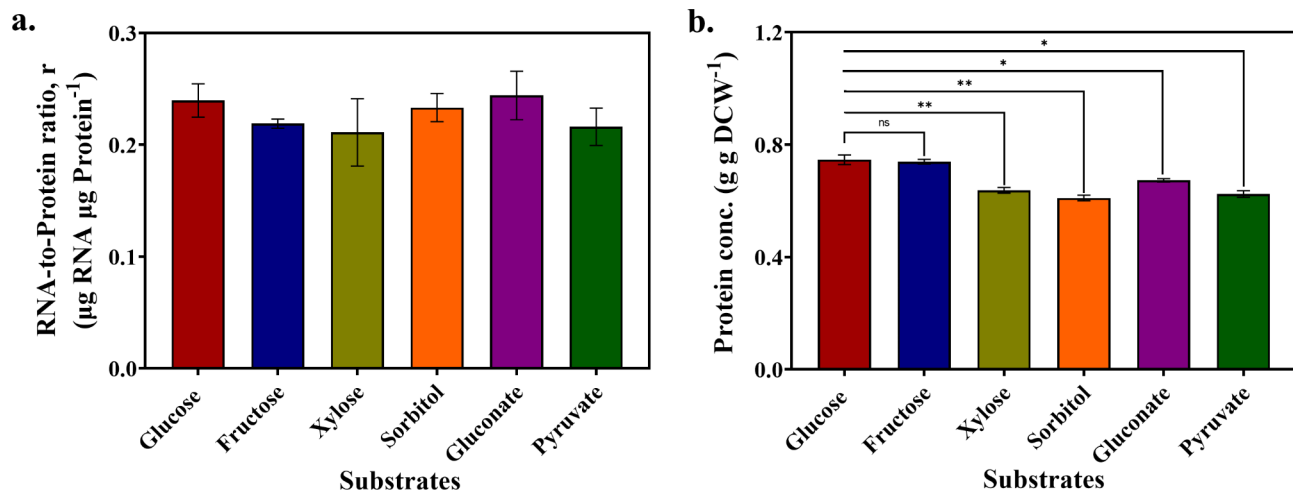


**Fig. 1** The cellular ribosomal abundances and its protein content. (a) The  $\frac{R}{P}$  ratio during anaerobic batch fermentation of different glycolytic and non-glycolytic substrates. (b) The total protein content during anaerobic growth of *E. coli* BW25113 on different substrates. The asterisks represent the level of significance as p-value < 0.05 (Student's t-test); ns: non-significant. The color codes representing the substrates in this figure are consistent throughout the manuscript

**Table 1** The theoretically calculated active ribosome fraction in *E. coli* BW25113 during anaerobic catabolism of different substrates

| Substrate | Growth rate, $\mu$ ( $\text{h}^{-1}$ ) | Active ribosome fraction, $f_{\text{active}}$ |
|-----------|--|---|
| Glucose   | $0.3096 \pm 0.0041$                    | $0.74 \pm 0.003$                              |
| Fructose  | $0.185 \pm 0.0025$                     | $0.61 \pm 0.004$                              |
| Xylose    | $0.0716 \pm 0.0073$                    | $0.36 \pm 0.025$                              |
| Sorbitol  | $0.0547 \pm 0.0032$                    | $0.3 \pm 0.013$                               |
| Gluconate | $0.2129 \pm 0.0046$                    | $0.65 \pm 0.006$                              |
| Pyruvate  | $0.0655 \pm 0.0053$                    | $0.34 \pm 0.019$                              |

gluconate, and pyruvate. However, there was no significant difference in ribosomal abundance during the fermentative breakdown of these substrates (Fig. 1 (a)). Contrarily, total cellular protein content significantly varied across substrates (except glucose and fructose had similar protein content) (Fig. 1 (b)). The substrates like xylose, sorbitol, gluconate, and pyruvate had total protein content comparatively lesser than glucose and fructose. Since ribosomes are protein-synthesizing machinery, we were intrigued by the non-significant difference in ribosomal abundance but a significant protein variation during the anaerobic fermentative catabolism of different substrates.

Also, *E. coli* cells exhibited unique specific growth rates in these culture conditions. The bacterial ribosomes play a key role in shaping its proliferation rate. Previously, a decline in the active ribosomal fraction was correlated with growth rate retardation [25]. To further understand the relationship between active ribosomal fraction and growth rate, we plotted active ribosomal content in *E. coli* at different growth rates from literature [25, 26]. Here, we observed a Michaelis-Menten type of relationship

between active ribosomal fraction and *E. coli* growth rate given as  $f_{\text{active}} = \frac{f_{\text{active}}^{\text{max}} \times \mu}{K_g + \mu}$ ; where  $f_{\text{active}}^{\text{max}}$  is the maximum fraction of active ribosomes in *E. coli* cells,  $K_g$  represents the bacterial growth rate corresponding to an active ribosomal fraction when it is exactly half of its maximum value, and  $\mu$  defines bacterial growth rate (See additional file 1, section S.1). As a result, we calculated the active ribosomal fraction which was responsible for different *E. coli* proliferation rates during anaerobic catabolism of glucose, fructose, xylose, sorbitol, gluconate, and pyruvate respectively (Table 1). At lower cell proliferation rates, the fraction of actively translating ribosomes declined, reducing cellular protein content. Next, we theoretically calculated the ribosomal translation elongation rate ( $k$ , amino acid per second) by using the formula  $k = \frac{(K_g + \mu) \times \sigma'}{f_{\text{active}}^{\text{max}} \times \frac{R}{P}}$ . It increased with the growth rate for maintaining the protein pool required for cellular maintenance and proliferation under nutrient-limited anaerobic growth (Additional file 1, Fig. S.1 (b)). Thus, the physiological outcome was a consequence of an interplay between active cellular ribosome content and translational elongation rate that eventually influenced bacterial cell proliferation rate.

#### The ratio of active to inactive ribosomal proteome determined cell proliferation rate

The cellular ribosomes as a protein translating entity, themselves require proteins (ribosomal and its affiliated proteins) for functionality. Consequently, the protein repertoire available for other cellular activity reduces. As ribosome-affiliated proteome fraction is directly linked to cellular ribosomal abundance ( $\frac{R}{P}$  ratio) (See additional

file 1, section S.2), the total ribosomal proteome share was similar during the metabolism of all six substrates (Fig. 2 (a)). However, active ribosomal proteome had the highest share during glucose catabolism, followed by

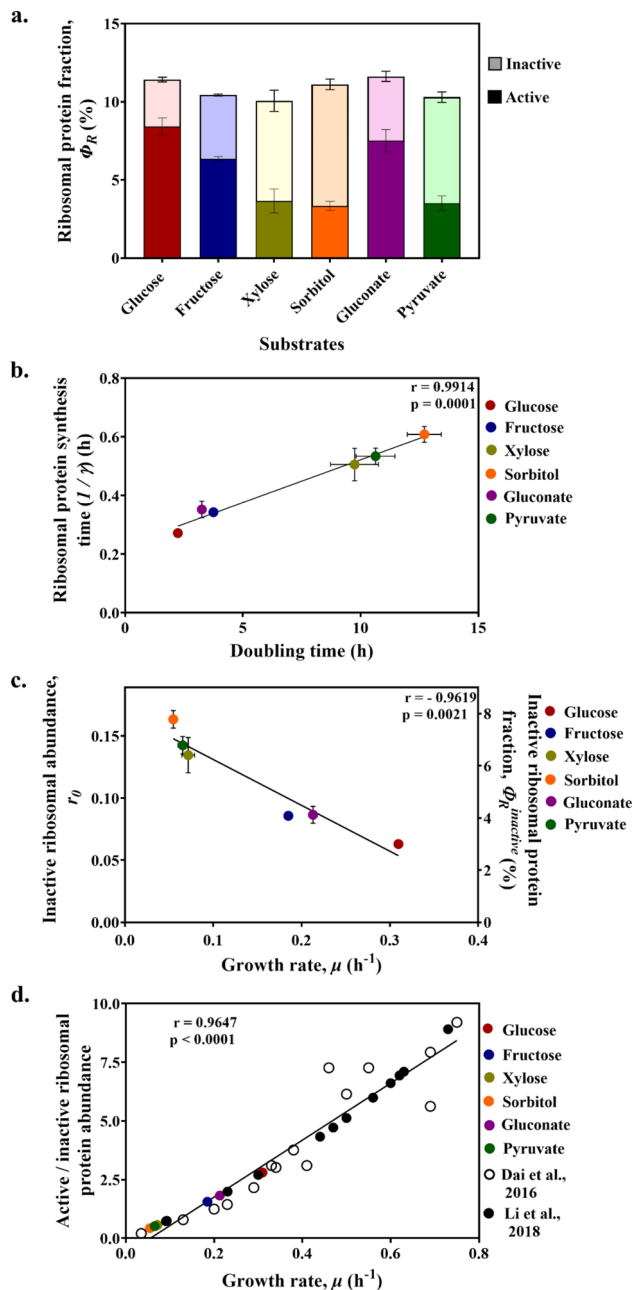


**Fig. 2** The role of the ribosomal-affiliated proteome in determining cell growth rate during the anaerobic fermentative breakdown of different glycolytic and non-glycolytic substrates. **(a)** The relative proportion of active and inactive ribosomal proteome share. **(b)** The influence of ribosomal protein synthesis time by a single ribosome, on cell doubling time. **(c)** The influence of inactive ribosomes and their affiliated proteome on cellular growth rate. **(d)** The relationship between the ratio of active-to-inactive ribosomal proteome abundance and cellular growth rate as obtained from this study and those calculated from literature data [3, 25]. The Pearson's  $r$  and  $p$  values indicate the level of significance;  $r > 0.8$  and  $p < 0.075$

gluconate and fructose metabolism. During the breakdown of xylose, sorbitol, and pyruvate, the inactive ribosomal proteome share increased, thereby imparting a retarded growth physiology.

The ribosomal protein synthesis time varied with cell doubling time (Fig. 2 (b)). Thus, the longer the time required to synthesize ribosomal proteins by a single ribosome, the slower the bacterial growth rate. During catabolism of substrates like xylose, pyruvate, and sorbitol, the actively translating ribosomes becomes limiting; which increases the ribosomal protein synthesis time thereby leading to growth retardation. As a result, the ribosomal protein synthesis time was a crucial determinant of *E. coli* BW25113 physiology during the anaerobic fermentative breakdown of glucose, fructose, xylose, sorbitol, gluconate, and pyruvate. Moreover, we observed a negative influence of inactive ribosomal abundance, along with inactive ribosomal proteome share on bacterial growth rate during anaerobic fermentative breakdown of different glycolytic and non-glycolytic substrates (Fig. 2 (c)). Thus, under nutrient-limited growth, a slow *E. coli* BW25113 growth rate can be attributed to a larger proportion of inactive ribosomal proteome. This can be the outcome of amino acid scarcity resulting from substrate catabolism in a minimal-growth medium. Additionally, an alternative to linear growth laws established previously [4, 25], we observed a direct influence of fractional active to inactive ribosomal proteome ratio on bacterial growth rate. This observation was supported by data consolidated from literature for *E. coli* cells [3, 25] proliferating in slow to medium growth regimes (growth rate  $< 0.8 h^{-1}$ ) (Fig. 2 (d)). Alternatively, this correlation even holds for the fractional ratio of active to inactive ribosomes for cells proliferating in the same regime. This is an interesting outcome of the study as it determines the extent to which ribosomes and their affiliated proteome can influence *E. coli* growth rate under nutrient-limited growth conditions.

#### The cost associated with catabolic sector proteome was determined by the substrate uptake mechanism and catabolism

For determining the proteome share associated with substrate influx during their anaerobic fermentative breakdown, we first calculated the associated proteome cost for the influx of each substrate. For each simulation, the experimentally determined metabolite secretion rates under anaerobic growth conditions were considered along with the parameters enlisted in additional file 1, section S.3. The experimentally determined substrate uptake rate was kept unbound while optimizing the growth rate. The catabolic proteome cost was determined by iterating value ranges 0 and 1 (100 iterations). The C-sector cost ( $w_C$ ) value corresponding to the predicted

substrate uptake rate and growth rate, that matched with experimentally determined values were considered. The study involved an equal number of carbons during anaerobic fermentation of all six substrates. As a result, the corresponding proportion of substrates varied, to compensate for the required carbon content in the growth medium. Depending upon variable substrate affinity and its uptake mechanism, the substrate influx rate and bacterial growth rate varied.

The bacterial cells had the least hindrance in pyruvate uptake (least uptake cost), owing to the dual uptake mechanism [27–29] operative in *E. coli* cells. However, its non-glycolytic catabolism failed to cope with optimal performance, giving slower proliferation rates. Next in line, was glucose internalization, followed by gluconate influx-associated cost. The substrate internalization rates for both substrates were similar, however, variation existed in bacterial growth rates due to different metabolic pathways. The xylose-associated influx cost was comparatively lower than fructose and sorbitol internalization. Although the uptake rate was decent, the bacterial proliferation rate was compromised here due to energy-intensive substrate conversions [30]. The fructose-associated cost was on the higher side with fructose being internalized slower than xylose. However, it supported a decent anaerobic bacterial growth rate. Lastly, sorbitol influx was a draining task for *E. coli* BW25113 cells that led to the lowest bacterial growth rate. Thus, theoretically calculated catabolism-associated proteome cost was an outcome of limiting substrate behavior comprising of substrate uptake rate, the substrate metabolic pathway, the cell proliferation rate, etc. (Table 2).

#### The nature of substrate influenced coarse-grained partitioning of *E. coli* proteome during anaerobic fermentative breakdown

The coarse-grained allocation of proteome into four functional sectors was done to understand how cellular resource partitioning shapes bacterial physiology. In *E. coli*, the core proteome share is independent of bacterial proliferation rate and constitutes 45% [4] of the total cellular proteome. The ribosomal proteome share was jointly calculated by experimentation and theoretical considerations. The relative active and inactive ribosomal

share is depicted alongside the housekeeping proteome sector (Fig. 3). Using the constrained allocation flux balance analysis, we were able to quantify the proteome cost associated with nutrient influx, thus the catabolic sector proteome was determined. Lastly, the metabolic sector proteome was grouped as the remaining cellular proteome and calculated as:

$$\varnothing_M = 1 - (\varnothing_Q + \varnothing_R + \varnothing_C)$$

The driving flux for the catabolic sector proteome was the substrate influx rate, where the relative distribution of the C-sector proteome varied with the type of substrate. The pyruvate influx occurred at the highest rate and its corresponding C-sector proteome constituted approximately 12% of the total cellular proteome. The substrates, glucose, and gluconate were internalized at similar rates, but their uptake mechanisms posed a difference in their catabolic proteome cost. This yielded different cell proliferation rates, and a slightly higher proteome was allocated for gluconate (~9%) influx as compared to glucose (~7%) uptake. For xylose internalization, ~15% proteome was channelized for its influx, whereas ~23% proteome was utilized for fructose influx. The highest catabolic proteome share was compromised for sorbitol influx (~29%). The catabolic proteome allocation for uptake of different substrates was a result of tuning between substrate affinity to *E. coli* cell, and its uptake mechanism.

Once the catabolic proteome resumes its activity, the remaining biosynthetic proteome also becomes functional for carrying out metabolic conversions, leading to cell growth and multiplication. A substantial allocation of proteome towards substrate uptake would render lesser proteome for cellular biosynthesis. As a result, the sorbitol metabolism accounted for the smallest metabolic proteome (~15%) share, implicating limited proteome allocation for supporting a moderate bacterial growth rate. The glucose (~37%) and gluconate (~34%) had comparatively higher biosynthetic proteome leading to higher cell proliferation rates. Next in line, was pyruvate biosynthetic proteome (~33%) capable of facilitating a higher cell proliferation rate. However, the metabolic pathway breakdown of pyruvate rendered insufficient energy biogenesis and redox level within the cell, which eventually

**Table 2** The theoretically calculated C-sector proteome cost in *E. coli* BW25113

| Substrate | Conc. (mM) | Substrate influx, $v_c$ (mM gDCW <sup>-1</sup> h <sup>-1</sup> ) | C-sector cost, $w_c$ (gDCW h mM <sup>-1</sup> ) | Growth rate, $\mu$ (h <sup>-1</sup> ) |
|-----------|------------|--|---|---------------------------------------|
| Glucose   | 11.11      | 14.35 ± 0.38   | 0.0048 ± 0.0011                                 | 0.3096 ± 0.0041                       |
| Fructose  | 11.11      | 9.1 ± 0.08   | 0.02523 ± 0.0                                   | 0.185 ± 0.0025                        |
| Xylose    | 13.33      | 11.43 ± 0.24   | 0.01263 ± 0.00183                               | 0.0716 ± 0.0073                       |
| Sorbitol  | 10.989     | 5.03 ± 0.18  | 0.05836 ± 0.00254                               | 0.0547 ± 0.0032                       |
| Gluconate | 11.002     | 14.17 ± 0.29   | 0.00649 ± 0.00142                               | 0.2129 ± 0.0046                       |
| Pyruvate  | 21.81      | 27.5 ± 0.32  | 0.00446 ± 0.0043                                | 0.0655 ± 0.0053                       |

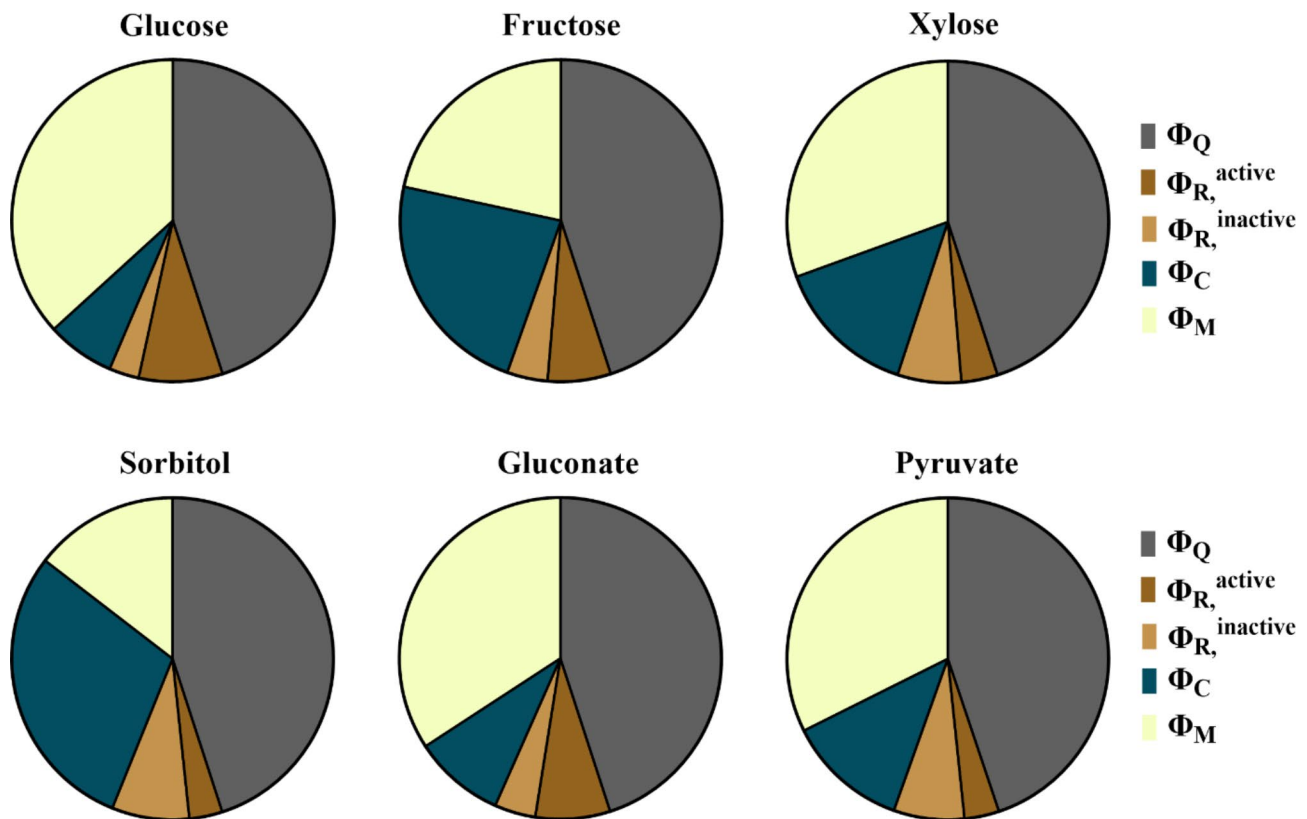


**Fig. 3** The proteome partitioning to different cellular functions during anaerobic batch fermentation of different substrates. The proteome fractions are named as:  $\Phi_Q$  - housekeeping (Q) sector,  $\Phi_{R, \text{active}}$  - active ribosomal (R) sector,  $\Phi_{R, \text{inactive}}$  - inactive ribosomal (R) sector,  $\Phi_C$  - catabolic (C) sector, and  $\Phi_M$  - metabolic (M) sector

compromised its growth rate. Moreover, similar was the case with xylose metabolism, where  $\sim 31\%$  of biosynthetic proteome was involved in shaping the bacterial physiology. However, the higher ATP requirement during substrate influx, compromised the ATP availability for other cellular functions, thereby lowering bacterial growth rate. Lastly, despite having a comparatively lesser metabolic proteome, the fructose ( $\sim 22\%$ ) metabolism was adequate to support decent bacterial growth.

#### The absolute quantification of proteins belonging to different coarse-grained sectors was correlated with physiological parameters

The housekeeping proteome occupies a fixed fraction in cellular proteome resources, invariant to the bacterial growth rate [4, 9]. This sector constitutes 0.45 fraction of *E. coli* proteome [4]. Upon quantifying the protein content of this sector, we found it to be linearly correlated with cell growth rate (Fig. 4 (a)). Thus, core proteome mass (by weight) responsible for cellular integrity and maintenance increased with the cell proliferation rate. The cell biomass yield with respect to substrate uptake rate was also linearly related to core protein mass (Fig. 4 (b)). This implies the influence of substrate influx rate on

core proteome mass. The higher the ratio of cell growth to the substrate, the higher the core proteome mass. Thus, the core cellular proteome is influenced by cell proliferation rate, wherein substrate influx and its catabolism play a vital role in determining the phenotypic outcome.

Also, the active ribosomal proteome abundance was positively correlated with bacterial proliferation rate and its corresponding biomass yield (Fig. 4 (a) and (b)). On the contrary, inactive ribosomal proteome abundance caused growth retardation, as it was negatively correlated with cellular growth rate and biomass yield (Fig. 4 (a) and (b)). Additionally, the fraction of active and inactive ribosomal abundances (by weight) was the determinant of cell growth rate and biomass yield for anaerobic batch fermentation of different substrates.

The substrate influx is a rate-limiting step, and the anabolic precursors are derivatives of substrate catabolism. Here, we observed a negative correlation between the substrate influx rate and the corresponding catabolic proteome abundance dedicated (Fig. 4 (c)). Thus, the higher the cellular substrate uptake rate, the lower the proteome expenditure on its transport and internalization. Similar was the behavior observed on substrate carbon internalization rate. The larger the carbon influx

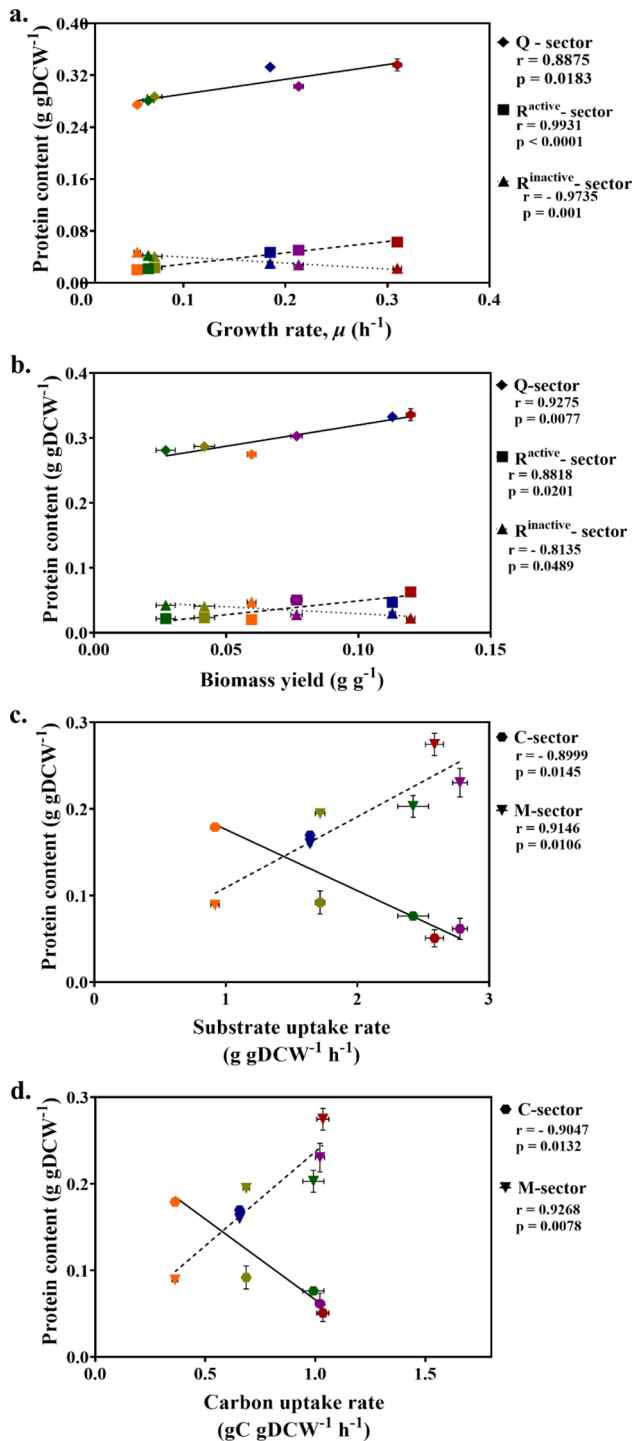


**Fig. 4** The role of cellular protein content in deciding the physiological outcomes. The correlation between the protein content of the house-keeping, and ribosomal sector with (a) Growth rate, and (b) Biomass yield. The relationship of catabolic, and metabolic proteome abundance with (c) Substrate uptake rate and (d) Carbon uptake rate

rate in the cell, the lower the protein expenditure (Fig. 4 (d)). However, the affinity of *E. coli* cells to the substrate can also become limiting over here. This is an interesting observation, as the basis of our study is equivalent carbon content. From this result the carbon content must not be the determinant of substrate influx in the cell, rather it's the type of substrate and its uptake mechanism that contribute to cell physiology.

The metabolic sector included biosynthetic proteins contributing to cellular metabolic activities. This sector had a lower span in substrates with a higher catabolic proteome sector. The higher expense of proteome on substrate internalization, rendered less proteome share for its metabolism, e.g. sorbitol catabolism. As a result, the growth rate was compromised. The biosynthetic sector proteome abundance showed a positive correlation with substrate influx rate and corresponding substrate-carbon influx rate, during anaerobic fermentation of different substrates (Fig. 4 (c) and (d)). This relationship established the substrate requirement for cellular metabolic functions. An influx of substrate at a lower rate would slow down cellular metabolic activities. Consequently, lower metabolic proteins would be channelized for carrying out the necessary cellular biosynthetic activities. As a result, the cell physiology would be compromised under such circumstances.

## Discussion

The cellular ribosomal abundance represented by RNA-to-protein ratio was high during anaerobic fermentation, as compared to aerobic growth conditions ( $\frac{R}{P}$  ratio  $< 0.2$ ) reported in the literature for similar growth regimes [3, 4, 25]. The cell cultivation under anoxic (oxygen stress) and fermentative (metabolic stress) conditions coupled with nutrient limitation would have rendered ribosomal content on the higher side. Dai et al., (2018) have also reported an increase in cellular ribosome content during hyperosmotic stress in exponentially proliferating *E. coli* cells. The cellular modulation of ribosomal abundance at different growth rates is unsurprisingly rate-limiting in *E. coli*, as established previously [4, 31]. Considering the anaerobic fermentative catabolism of substrates, the relative proportion of actively translating and non-active ribosomes was critical in determining the *E. coli* growth rate. The fraction of translating ribosomes declined at slower growth rates, which increased the burden on *E. coli* BW25113 cells for optimal behavior. Additionally, under nutrient-limited conditions, the bacterial cell doubling time is largely influenced by the time taken by a single ribosome to translate all of its proteins. The ribosomes are rendered functional only when rRNA and its affiliated proteins are in an active state. The translation rate of amino acids into ribosomal proteins serves as a

key determinant of protein synthesis and biomass accumulation, which eventually impacts the bacterial growth rate and its cell doubling time. This, in turn, depends on the ribosome's translational capacity and elongation rate determined by the induction of secondary messenger-like - ppGpp mediated response in a nutrient-limited medium [25, 31, 32]. In *E. coli*, a high ppGpp level is triggered by the enzyme RelA [33], upon accumulation of deacylated tRNAs at the ribosomal A – site, which enables the cell to adjust its ribosomal content. Also, ppGpp has been reported to inhibit the initiation of DNA replication and its supercoiling near the origin of replication [34, 35], or ppGpp along its co-regulator DksA represses the rRNA synthesis and the gene expression of ribosome affiliated proteins [36, 37]. Therefore, the ppGpp overproduction lowers the bacterial growth rate and enhances the stress tolerance in *E. coli* under harsh growth environments [38]. Under such circumstances, the resource re-allocation occurs from ribosome synthesis to stress response [38], mostly metabolic [32] and catabolic activities under nutrient-limited conditions (Fig. 3). Interestingly, in nutrient-limited growth, the proteome efficiency increases along nutrient pathway flow, where substrate uptake and metabolism seem to be less efficient while amino acid biosynthesis and translation utilize proteome efficiently [39]. Our observations regarding the higher share of catabolic and metabolic proteome sectors during nutrient- and oxygen-stressed fermentative growth of *E. coli*, are on par with previously reported outcomes. Additionally, the low ATP level during anaerobic fermentation facilitates a decline in rRNA synthesis [40]. Due to the translational feedback inhibition, the amount of free ribosomal protein inhibits their mRNA, which results in a decline in ribosomal protein synthesis at lower energy levels during anaerobic fermentation. This leads to an increased proportion of inactive ribosomes, along with the active ribosomes translating at a decreased elongation rate. Eventually, *E. coli* cells exhibit slower growth rates and increased ribosomal abundance [26] during anoxic batch fermentation.

Moving beyond ribosomal dynamics, the nature of substrate metabolism also emerges as a significant determinant of *E. coli*'s physiological response. In anaerobic batch fermentation of glucose, fructose, xylose, sorbitol, gluconate, and pyruvate, the nature of substrate metabolism becomes limiting in providing the requisite energy level for cellular ribosomal activities. Thus, dictating the allocation of cellular resources, impacting ribosomal translation capacity, protein synthesis times, and ultimately, cell doubling rates. In addition, our study identified a modification of the established bacterial growth law, wherein we observed that the relative proportion of active to inactive ribosomes, or the abundance of ribosomal proteins, had a linear impact on bacterial growth rate under

conditions of slow proliferation. This can form the basis for studying cell physiology under different growth conditions and understanding the ribosomal impact on the resulting phenotype. A critical bottleneck in cell survivability is substrate influx into the cellular environment. This substrate internalization process could be energy consuming, like for xylose influx, or the *E. coli* host can possess a low affinity for substrate like sorbitol, thereby declining the growth rate. Alternatively, the substrate uptake would happen at a comparatively lower pace like fructose, but cellular metabolic wiring would favor a substantial proliferation rate. Under such circumstances, the carbon catabolic proteome share would increase, thereby limiting the proteome resource for other cellular activities. Similar observations have been reported for different modes of metabolic limitations [1, 14]. The substrates like glucose, gluconate, and pyruvate were internalized at a higher rate, thus accounting for lower proteome share. However, we couldn't generalize the relationship between substrate influx rate, catabolic proteome allocation, and corresponding growth rate. As these parameters are substrate-specific, cells behave differently under different growth environments. However, if substrate influx happened at a higher rate, then lower catabolic proteome share would be allocated for its internalization. Consequently, *E. coli* cells would have a higher proteome share for other metabolic activities, thereby improving their performance under different growth conditions.

The core proteome abundance involved in cellular maintenance increased linearly with *E. coli* growth rate. To sustain a higher proliferation rate, the bacterial cell expended higher cellular proteome resources on its housekeeping activities. However, the housekeeping proteome fraction remained unaltered across different growth environments. The active ribosomal abundance facilitated bacterial growth rate and biomass yield. However, the opposite was the influence of inactive ribosomal abundance on growth rate and biomass yield. The biosynthetic proteome plays a crucial role in maintaining flux across metabolic networks operative in *E. coli* cells. These metabolic proteins regulated intermediate bio-conversions necessary for the polymerization of macromolecules and cellular energy states. Moreover, the metabolic proteome abundance allocated for such cellular activities was largely determined by the substrate influx rate. The higher the substrate internalization rate, the more would be the biosynthetic proteome requirement to provide precursors for macromolecule polymerization.

## Conclusions

In conclusion, this study elucidates the phenotypic variations resulting from anoxic catabolism of different glycolytic and non-glycolytic substrates by *E. coli*. The critical wiring between host native metabolism and its proteome

allocation for different cellular activities was influenced by the nature of catabolic substrates resulting in distinct phenotypes. The rate-limiting steps like substrate uptake, active ribosomal abundance and translation rate, proteome partitioning, etc. determined the cell-specific growth rate under nutrient-limited anoxic conditions. These insights advance our understanding of *E. coli* adapting to anaerobic fermentative growth under limited resources. This knowledge of anaerobic metabolism can be explored in understanding the microbial metabolism regulation and efficient management of cellular resources, for sustainable bioprocessing. Future studies can be built upon these findings by exploring ribosomal profiling by improving nutritional capacity or undertaking metabolomic and proteomic studies for elaborating the impact of key metabolic reactions and proteome cost associated with bacterial physiology across different mediums in an anoxic environment. This can make the findings more pronounced and valuable to scientific communities. Overall, this study recognizes that phenotypic outcomes under different growth conditions are manifestations of altered regulatory controls, including metabolic rewiring and proteome rearrangement. A comprehensive understanding can give better control over biological conversions and desired phenotypes, thereby minimizing the cost associated with product-driven bioconversions.

### Supplementary Information

The online version contains supplementary material available at <https://doi.org/10.1186/s12934-025-02658-4>.

Supplementary Material 1

### Acknowledgements

Not applicable.

### Author contributions

H.M. and V.K.V. conceived the idea and designed the experiments. H.M. performed experiments and theoretical simulations. H.M., D.A., and V.K.V. analyzed the experimental and theoretical data. H.M. wrote the original draft. H.M., D.A. and V.K.V. reviewed and finalized the paper.

### Funding

This work was supported by the Department of Biotechnology (DBT) – India grant BT/PR13713/BBE/117/83/2015 received to Prof. Venkatesh K. V (PI) and Dr. Deepti Appukuttan (Co-PI). Huda Momin is thankful to DBT – India and Industrial Research and Consultancy Center – Indian Institute of Technology Bombay for supporting her fellowship.

### Data availability

No datasets were generated or analysed during the current study.

### Declarations

#### Ethics approval and consent to participate

Not applicable.

#### Consent for publication

Not applicable.

### Competing interests

The authors declare no competing interests.

Received: 5 December 2024 / Accepted: 20 January 2025

Published online: 25 March 2025

### References

1. You C, Okano H, Hui S, Zhang Z, Kim M, Gunderson CW, et al. Coordination of bacterial proteome with metabolism by cyclic AMP signalling. *Nature*. 2013;500(7462):301–6.
2. Li GW, Burkhardt D, Gross C, Weissman JS. Quantifying absolute protein synthesis rates reveals principles underlying allocation of cellular resources. *Cell*. 2014;157(3):624–35.
3. Li SHJ, Li Z, Park JO, King CG, Rabinowitz JD, Wingreen NS, et al. *Escherichia coli* translation strategies differ across carbon, nitrogen and phosphorus limitation conditions. *Nat Microbiol*. 2018;3(8):939–47.
4. Scott M, Gunderson CW, Mateescu EM, Zhang Z, Hwa T. Interdependence of Cell Growth. *Science* (1979). 2010;330(6007):1099–102.
5. Bremer H, Dennis PP. Modulation of Chemical composition and other parameters of the cell at different exponential growth rates. *EcoSal Plus*. 2008;3(5.2.3):1–48.
6. Klumpp S, Zhang Z, Hwa T. Growth rate-Dependent Global effects on Gene expression in Bacteria. *Cell*. 2009;139(7):1366–75.
7. Basan M. Resource allocation and metabolism: the search for governing principles. *Curr Opin Microbiol*. 2018;45:77–83.
8. Scott M, Klumpp S, Mateescu EM, Hwa T. Emergence of robust growth laws from optimal regulation of ribosome synthesis. *Mol Syst Biol*. 2014;10(8):747.
9. Scott M, Hwa T. Bacterial growth laws and their applications. *Curr Opin Biotechnol*. 2011;22(4):559–65.
10. Nomura M, Gourse R, Baughman G. Regulation of the synthesis of ribosomes and ribosomal components. *Ann RevBiochem*. 1984;53:75–117.
11. Kostinski S, Reuveni S. Ribosome composition maximizes Cellular Growth Rates in *E. Coli*. *Phys Rev Lett*. 2020;125(2):028103.
12. Neidhardt FC, Magasanik B. Studies on the role of ribonucleic acid in the growth of bacteria. *Biochim Biophys Acta*. 1959;42(2):99–116.
13. Schaechter M, Maaloe O, Kjeldgaard N. Dependency on medium and temperature of cell size and chemical composition during balanced growth of *Salmonella typhimurium*. *J Gen Microbiol*. 1958;19:592–606.
14. Hui S, Silverman JM, Chen SS, Erickson DW, Basan M, Wang J, et al. Quantitative proteomic analysis reveals a simple strategy of global resource allocation in bacteria. *Mol Syst Biol*. 2015;11(2):784.
15. Peebo K, Valgepea K, Maser A, Nahku R, Adamberg K, Vilu R. Proteome reallocation in *Escherichia coli* with increasing specific growth rate. *Mol Biosyst*. 2015;11(4):1184–93.
16. Schmidt A, Kochanowski K, Vedelaar S, Ahrné E, Volkmer B, Callipo L, et al. The quantitative and condition-dependent *Escherichia coli* proteome. *Nat Biotechnol*. 2016;34(1):104–10.
17. Basan M, Hui S, Okano H, Zhang Z, Shen Y, Williamson JR, et al. Overflow metabolism in *Escherichia coli* results from efficient proteome allocation. *Nature*. 2015;528(7580):99–104.
18. O'Brien EJ, Monk JM, Palsson BO. Using genome-scale models to predict biological capabilities. *Cell*. 2015;161(5):971–87.
19. Mori M, Hwa T, Martin OC, De Martino A, Marinari E. Constrained allocation flux balance analysis. *PLoS Comput Biol*. 2016;12(6):1–24.
20. Mori M, Marinari E, De Martino A. A yield-cost tradeoff governs *Escherichia coli*'s decision between fermentation and respiration in carbon-limited growth. *NPJ Syst Biol Appl*. 2019;5(1).
21. Zeng H, Yang A. Modelling overflow metabolism in *Escherichia coli* with flux balance analysis incorporating differential proteomic efficiencies of energy pathways. *BMC Syst Biol*. 2019;13(1):1–18.
22. Grenier F, Matteau D, Baby V, Rodrigue S. Complete genome sequence of *Escherichia coli* BW25113. *Genome Announc*. 2014;2(5):e01038–14.
23. Invitrogen. TRIZOL® user guide. ThermoFisher Sci. 2020;0(15596026):2–5.
24. Orth JD, Conrad TM, Na J, Lerman JA, Nam H, Feist AM, et al. A comprehensive genome-scale reconstruction of *Escherichia coli* metabolism-2011. *Mol Syst Biol*. 2011;7(535):1–9.
25. Dai X, Zhu M, Warren M, Balakrishnan R, Patsalo V, Okano H et al. Reduction of translating ribosomes enables *Escherichia coli* to maintain elongation rates during slow growth. *Nat Microbiol*. Dec. 2016;2:16231.

26. Dai X, Zhu M, Warren M, Balakrishnan R, Okano H, Williamson JR et al. Slowdown of translational elongation in *Escherichia coli* under hyperosmotic stress. *mBio*. 2018;9(1).
27. Kornberg HL, Smith J. Genetic control of the uptake of pyruvate by *Escherichia coli*. *BBA - Gen Subj*. 1967;148(2):591–2.
28. Lang VJ, Leystra-Lantz C, Cook RA. Characterization of the specific pyruvate transport system in *Escherichia coli* K-12. *J Bacteriol*. 1987;169(1):380–5.
29. Kreth J, Lengeler JW, Jahreis K. Characterization of pyruvate uptake in *Escherichia coli* K-12. *PLoS ONE*. 2013;8(6):6–12.
30. Hasona A, Kim Y, Healy FG, Ingram LO, Shanmugam KT. Pyruvate formate lyase and acetate kinase are essential for anaerobic growth of *Escherichia coli* on xylose. *J Bacteriol*. 2004;186(22):7593–600.
31. Belliveau NM, Chure G, Hueschen CL, Garcia HG, Kondev J, Fisher DS, et al. Fundamental limits on the rate of bacterial growth and their influence on proteomic composition. *Cell Syst*. 2021;12(9):924–e9442.
32. Zhu M, Dai X. Growth suppression by altered (p)ppGpp levels results from non-optimal resource allocation in *Escherichia coli*. *Nucleic Acids Res*. 2019;47(9):4684–93.
33. Hauryliuk V, Atkinson GC, Murakami KS, Tenson T, Gerdes K. Recent functional insights into the role of (p)ppGpp in bacterial physiology. *Nature Reviews Microbiology*. Nature Publishing Group. 2015;13:298–309.
34. Kraemer JA, Sanderlin AG, Laub MT. The stringent response inhibits DNA replication initiation in *E. Coli* by modulating supercoiling of *oric*. *mBio*. 2019;10(4).
35. Fernández-Coll L, Maciag-Dorszynska M, Tailor K, Vadia S, Levin PA, Szalewska-Palasz A et al. The absence of (P)ppGpp renders initiation of *Escherichia coli* chromosomal DNA synthesis independent of growth rates. *mBio*. 2020;11(2).
36. Paul BJ, Barker MM, Ross W, Schneider DA, Webb C, Foster JW et al. DksA: A Critical Component of the Transcription Initiation Machinery that Potentiates the Regulation of rRNA Promoters by ppGpp and the Initiating NTP. *Cell*. 2004:118.
37. Jin DJ, Cagliero C, Zhou YN. Growth rate regulation in *Escherichia coli*. 36, *FEMS Microbiology Reviews*. 2012:269–87.
38. Zhu M, Mu H, Dai X. Integrated control of bacterial growth and stress response by (p)ppGpp in *Escherichia coli*: a seesaw fashion. *iScience*. 2024;27(2).
39. Hu XP, Schroeder S, Lercher MJ. Proteome efficiency of metabolic pathways in *Escherichia coli* increases along the nutrient flow. *mSystems*. 2023;8(5).
40. Kramer G, Sprenger RR, Nessen MA, Roseboom W, Speijer D, De Jong L, et al. Proteome-wide alterations in *Escherichia coli* translation rates upon anaerobiosis. *Mol Cell Proteomics*. 2010;9(11):2508–16.

### Publisher's note

Springer Nature remains neutral with regard to jurisdictional claims in published maps and institutional affiliations.